

# Morphologic and molecular analysis of liver injury after SARS-CoV-2 vaccination reveals distinct characteristics

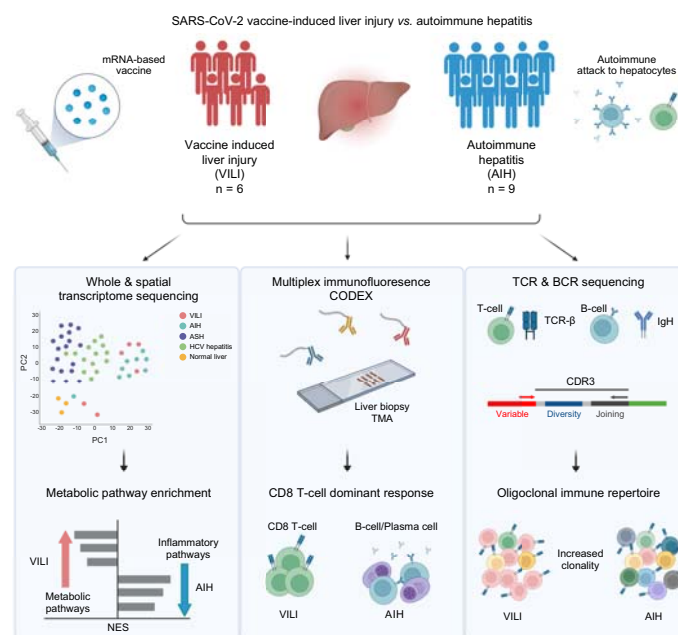
## Authors

Sarp Uzun, Carl P. Zinner, Amke C. Beenen, ..., Alexandar Tzankov, Benedetta Terziroli Beretta-Piccoli, Matthias S. Matter

## Correspondence

matthias.matter@usb.ch (M.S. Matter).

## Graphical abstract



## Highlights

- Vaccine-induced liver injury demonstrates similarities to autoimmune hepatitis but also distinct differences.
- Vaccine-induced liver injury shows enrichment in mitochondrial metabolism and oxidative stress-related pathways.
- Vaccine-induced liver injury is dominated by CD8<sup>+</sup> T cell infiltrates.
- Vaccine-induced liver injury presents oligoclonal immune responses and distinct T-cell receptor beta chain usage.

## Impact and implications

Little is known about the pathophysiology of COVID-19 vaccine-induced liver injury (VILI). Our analysis shows that COVID-19 VILI shares some similarities with autoimmune hepatitis, but also has distinct differences such as increased activation of metabolic pathways, a more prominent CD8<sup>+</sup> T cell infiltrate, and an oligoclonal T and B cell response. Our findings suggest that VILI is a distinct disease entity. Therefore, there is a good chance that many patients with COVID-19 VILI will recover completely and will not develop long-term autoimmune hepatitis.

# Morphologic and molecular analysis of liver injury after SARS-CoV-2 vaccination reveals distinct characteristics

Sarp Uzun<sup>1</sup>, Carl P. Zinner<sup>1</sup>, Amke C. Beenen<sup>1</sup>, Ilaria Alborelli<sup>1</sup>, Ewelina M. Bartoszek<sup>2</sup>, Jason Yeung<sup>3</sup>, Byron Calgua<sup>1</sup>, Matthias Reinscheid<sup>4,5</sup>, Peter Bronsert<sup>6,7</sup>, Anna K. Stalder<sup>1</sup>, Jasmin D. Haslbauer<sup>1</sup>, Juerg Vosbeck<sup>1</sup>, Luca Mazzucchelli<sup>8</sup>, Tobias Hoffmann<sup>9</sup>, Luigi M. Terracciano<sup>10,11</sup>, Gregor Hutter<sup>12,13</sup>, Michael Manz<sup>14</sup>, Isabelle Panne<sup>14</sup>, Tobias Boettler<sup>4</sup>, Maike Hofmann<sup>4</sup>, Bertram Bengsch<sup>4,15,16</sup>, Markus H. Heim<sup>14,17</sup>, Christine Bernsmeier<sup>14,17</sup>, Sizun Jiang<sup>3,18,19</sup>, Alexandar Tzankov<sup>1</sup>, Benedetta Terziroli Beretta-Piccoli<sup>20,21,22</sup>, Matthias S. Matter<sup>1,\*</sup>

Journal of Hepatology 2023. vol. 79 | 666–676



**Background & Aims:** Liver injury after COVID-19 vaccination is very rare and shows clinical and histomorphological similarities with autoimmune hepatitis (AIH). Little is known about the pathophysiology of COVID-19 vaccine-induced liver injury (VILI) and its relationship to AIH. Therefore, we compared VILI with AIH.

**Methods:** Formalin-fixed and paraffin-embedded liver biopsy samples from patients with VILI (n = 6) and from patients with an initial diagnosis of AIH (n = 9) were included. Both cohorts were compared by histomorphological evaluation, whole-transcriptome and spatial transcriptome sequencing, multiplex immunofluorescence, and immune repertoire sequencing.

**Results:** Histomorphology was similar in both cohorts but showed more pronounced centrilobular necrosis in VILI. Gene expression profiling showed that mitochondrial metabolism and oxidative stress-related pathways were more and interferon response pathways were less enriched in VILI. Multiplex analysis revealed that inflammation in VILI was dominated by CD8<sup>+</sup> effector T cells, similar to drug-induced autoimmune-like hepatitis. In contrast, AIH showed a dominance of CD4<sup>+</sup> effector T cells and CD79a<sup>+</sup> B and plasma cells. T-cell receptor (TCR) and B-cell receptor sequencing showed that T and B cell clones were more dominant in VILI than in AIH. In addition, many T cell clones detected in the liver were also found in the blood. Interestingly, analysis of TCR beta chain and Ig heavy chain variable-joining gene usage further showed that TRBV6-1, TRBV5-1, TRBV7-6, and IgHV1-24 genes are used differently in VILI than in AIH.

**Conclusions:** Our analyses support that SARS-CoV-2 VILI is related to AIH but also shows distinct differences from AIH in histomorphology, pathway activation, cellular immune infiltrates, and TCR usage. Therefore, VILI may be a separate entity, which is distinct from AIH and more closely related to drug-induced autoimmune-like hepatitis.

© 2023 The Author(s). Published by Elsevier B.V. on behalf of European Association for the Study of the Liver. This is an open access article under the CC BY license (<http://creativecommons.org/licenses/by/4.0/>).

## Introduction

Severe acute respiratory syndrome coronavirus 2 (SARS-CoV-2), the causative agent of coronavirus disease 2019 (COVID-19), has infected millions of people worldwide with a great socio-economic impact.<sup>1</sup> The most effective strategy to reduce morbidity and mortality from SARS-CoV-2 infection is the development of safe and effective vaccines. Several different COVID-19 vaccines have been approved and millions of people have received a dose to date.<sup>2</sup> Since the introduction of COVID-19 vaccines, potential adverse events have been reported. Most of them are mild and include local symptoms, fatigue, fever, headache, and myalgia.<sup>2</sup> Rarely, COVID-19 vaccination has been associated with autoimmune disorders such as myocarditis, immune thrombocytopenia, and Guillain-Barré syndrome.<sup>2</sup>

In addition, several recent reports have described hepatitis following COVID-19 vaccination as a very rare event and supported a direct correlation.<sup>3–11</sup> Multiple potential mechanisms of COVID-19 vaccine-related tissue injury have been suggested, including molecular mimicry, triggering of a latent autoimmune disease, vaccine-induced specific antibody production, bystander activation with polyclonal B cell expansion, epitope spreading, and the effects of particular adjuvants.<sup>2,12–14</sup>

COVID-19 vaccine-induced liver injury (VILI) resembles autoimmune hepatitis (AIH) clinically, biochemically, morphologically and, to some extent, also serologically.<sup>10,11,15</sup> Many, but not all, patients with VILI fulfil the criteria for the diagnosis of AIH.<sup>10,11,16,17</sup> However, it is not known whether hepatitis following COVID-19 vaccination is a form of triggered AIH or

Keywords: Autoimmune hepatitis; COVID-19; Drug-induced liver injury; SARS-CoV-2; Vaccination.

Received 17 August 2022; received in revised form 10 May 2023; accepted 19 May 2023; available online 7 June 2023

\* Corresponding author. Address: Institute of Pathology, University Hospital Basel, Basel, Schoenbeinstrasse 40, CH-4031 Basel, Switzerland. Tel.: +41 61 328 64 71.

E-mail address: [matthias.matter@usb.ch](mailto:matthias.matter@usb.ch) (M.S. Matter).

<https://doi.org/10.1016/j.jhep.2023.05.020>



ELSEVIER

whether it rather belongs to a condition described as drug-induced autoimmune-like hepatitis (DI-AIH).<sup>18,19</sup> Furthermore, very little is known about the pathophysiology of this phenomenon.<sup>20</sup>

In this study, we aimed to characterise the morphological and molecular features of VILI and compare them with those of patients with AIH. By using gene expression profiling, immune repertoire sequencing, and multiplex immunofluorescence we show that both entities share some features but also have distinct differences.

## Materials and methods

The materials and methods can be found in the supplementary documents online.

### Ethical statement

The study was approved by the ethics commission of Northern Switzerland (EKNZ; study ID: 2020-00969), the ethics commission at the Albert-Ludwigs-University, Germany and the Comitato Etico cantonale Ticino, Switzerland. All tissue samples were collected as part of the routine diagnostic workup and selected retrospectively, informed consent was obtained from all vaccinated patients, and the study was conducted according to the Declaration of Helsinki (1975).

## Results

### Characteristics of study and control cohort

In our study, we included formalin-fixed and paraffin-embedded (FFPE) liver biopsies from six patients with COVID-19 VILI (Table 1, Tables S1, and S2). All patients received mRNA-1273 from Moderna, the vaccine most commonly administered in Switzerland. Two patients have been described in previous publications.<sup>6,11</sup> Average patient age was 58 (range 21–85 years). Two patients were female and four were male. Three patients developed symptoms after the first vaccination and three after the second. The main symptoms were fatigue, jaundice, and nausea. The time to symptom onset varied from 2 to 28 days after vaccination. Patients did not have autoimmune diseases, except for one patient (VILI3), who had a history of elevated antibodies against thyroid peroxidase and polymyalgia. All patients were negative by PCR or antibody testing for viral hepatitis (hepatitis A, B, C, D, and E) and none of the patients had a history of clinically apparent COVID-19 disease. At the time of vaccination, two patients were taking several medications for concomitant diseases for more than 5 years (VILI5: aspirin, rosuvastatin, metformin;

VILI6: lercanidipine, telmisartan). One patient had been taking oral contraceptives for 3 years and took herbal medicines for a short time a few months before vaccination. One patient regularly took multivitamin supplements. The remaining two patients have not taken any medicine. None of the patients had any prior history of liver disease or alcohol abuse. After the liver biopsy, five patients received prednisone. One patient did not receive any treatment. All patients improved and remained in remission during the follow-up period (Table 1).

Because VILI resembles AIH,<sup>10,11</sup> we selected archived FFPE liver biopsies from untreated patients with Type 1 AIH (n = 9) for comparison, which were taken at the time of initial diagnosis of AIH and early after appearance of symptoms (Tables S1 and S2). Patients with AIH were on average 61 years old (range 49–78 years) and were predominantly female (n = 8).

### Clinical and histological comparison

Serum liver enzyme levels (aspartate aminotransferase [AST], alanine aminotransferase [ALT], gamma-glutamyl transferase [GGT], alkaline phosphatase [ALP], and bilirubin) were increased in both cohorts. In comparison with patients with AIH, VILI showed higher levels of AST, ALT, and bilirubin, but lower levels of GGT and ALP, without reaching statistical significance (Tables S1 and S2). Liver injury calculated with the R ratio<sup>21</sup> was hepatocellular in all patients with VILI and AIH, except for one patient with AIH, who had mixed, hepatocellular, and cholestatic liver injury. Serum autoantibodies in the VILI cohort showed anti-nuclear antibodies (ANAs) in three cases, of whom one additionally showed atypical anti-mitochondrial antibodies (AMAs); one patient showed elevated anti-actin antibodies (AAAs) only (Tables S1 and S2). Therefore, four out of six (67%) patients with VILI were ANA or AAA positive. In the AIH cohort, seven patients were ANA positive, two of them in conjunction with elevated anti-smooth muscle antibodies (ASMA) or AAA. Two additional patients had either elevated ASMA or AAA only. Therefore, all patients from the AIH cohort showed elevated ANA and/or elevated ASMA/AAA. Anti-soluble liver antigen (anti-SLA), anti-liver-kidney microsome 1 (anti-LKM1), and anti-liver cytosol type 1 (anti-LC1) were negative in all patients from both cohorts. Two patients with AIH also showed anti-neutrophil cytoplasmic antibodies (ANCAs). IgG levels were increased in two out of the five tested patients with VILI, and in four out of eight tested patients with AIH.

After the appearance of symptoms, all patients underwent liver biopsy (2–90 days after symptoms for VILI and 9–150 days for AIH) and histological analysis according to current recommendations.<sup>22–24</sup> Variable degrees of piecemeal necrosis, focal

**Table 1. Cohort of patients with liver injury after COVID-19 vaccination.**

| Patient ID | Age | Sex | Symptoms                       | Symptoms after vaccination     | Drugs at time of vaccination     | Therapy (prednisone)* | Follow-up (months) | Remission |
|------------|-----|-----|--------------------------------|--------------------------------|----------------------------------|-----------------------|--------------------|-----------|
| VILI1      | 48  | F   | Fatigue, abdominal pain        | 2 days after 2nd vaccination   | Multivitamins                    | 40 mg/d for 3 months  | 18                 | Yes       |
| VILI2      | 85  | M   | Nausea, dark urine             | 5 days after 1st vaccination   | None                             | None                  | 18                 | Yes       |
| VILI3      | 21  | F   | Fatigue, jaundice, nausea      | 21 days after 2nd vaccination  | Oral contraceptive               | 60 mg/d for 3 months  | 15                 | Yes       |
| VILI4      | 53  | M   | Fatigue, jaundice, nausea      | 7 days after 2nd vaccination   | None                             | 40 mg/d for 3 months  | 18                 | Yes       |
| VILI5      | 63  | M   | Fatigue, jaundice, weight loss | 10 days after 1st vaccination  | Aspirin, rosuvastatin, metformin | 40 mg/d for 11 months | 18                 | Yes       |
| VILI6      | 78  | M   | None                           | 28 days after 1st vaccination† | Lercanidipine, telmisartan       | 40 mg/d for 5 months  | 12                 | Yes       |

\*Initial dose, reduced thereafter according to liver enzyme levels and/or clinical course.

†Only elevated liver enzymes.

lytic necrosis/apoptosis/inflammation, and portal inflammation were found without significant differences between the two cohorts (Tables S1, S3, and Fig. S1). In contrast, confluent necrosis was more extensive in VILI ( $p = 0.0025$ ). The summarised Ishak grading score<sup>24</sup> was similar in both cohorts and between 3 and 16 (average 12.2) in patients with VILI and 6 to 14 (average 10.3) in patients with AIH. In all patients with VILI and five patients with AIH no fibrosis was found, corresponding to Ishak stage 0. Four patients with AIH presented with stage 1 fibrosis. Rosette formation, emperipolesis, endothelialitis, and cholestasis were frequently found in both cohorts.<sup>22,23</sup> Bile duct injury was present in only one patient of the VILI cohort and two patients of the AIH cohort. None of the patients showed steatosis. Likewise, there was no difference in the number of eosinophils between both cohorts.

In summary, histological analysis revealed a diagnosis of likely AIH in five out of six patients with VILI and a diagnosis of possible AIH in one patient according to the most recent recommendations.<sup>23</sup> Moreover, three out of five patients with VILI had a probable/definite AIH score according to the simplified AIH criteria (Table S1).<sup>17</sup> For one patient with VILI, not all values were available for calculation. In contrast, all patients with AIH showed histologically the diagnosis of a likely AIH and a probable/definite AIH score according to the simplified criteria.

#### Patients with VILI and AIH have related but clearly different gene expression profiles

To understand the different biological mechanisms between VILI and AIH, we performed whole transcriptome profiling with bulk RNA, isolated from FFPE liver biopsies of patients with VILI and AIH. As further controls, we added liver biopsies from patients with alcoholic steatohepatitis (ASH;  $n = 17$ ) and chronic HCV infection ( $n = 13$ ). Patients with HCV were untreated and showed high viral load at the time of biopsy. The average patient age was 64.3 years for ASH and 58.3 years for HCV, and both cohorts had cirrhotic liver disease (Table S4). Additionally, we included three patients with histologically normal liver tissue, who presented with a metastasis to the liver (two with pancreatic and one with urothelial carcinoma) (Table S4).

Principal component analysis showed that patients with VILI and AIH had different transcriptome profiles but were close to each other and significantly different from patients with chronic HCV infection or ASH (Fig. 1A). Two patients with VILI (#1 and #2) and one patient with AIH (#7) clustered close to normal liver samples. Interestingly, all of these three patients had little inflammation signature according to RNA transcriptome (see Fig. 2A below). Differential gene expression analysis revealed 70 genes (43 upregulated and 27 downregulated) that showed a significant difference between the VILI and AIH cohort (log fold change [lfc]  $>0.58$ ,  $p_{\text{adj}} < 0.05$ ) (Fig. 1B and Table S5). To validate our gene expression profiling data, we selected one significantly upregulated and one significantly downregulated gene and performed a qPCR. As an upregulated gene we selected *TSPAN8* (lfc = 2.172,  $p_{\text{adj}} = 0.002$ ), which has been shown to correlate with SARS-CoV-2 infection rate,<sup>25</sup> and *RNF213* (lfc = -0.793,  $p_{\text{adj}} = 0.026$ ), associated with immune response and interferon signalling.<sup>26</sup> Expression changes were confirmed by qPCR for both genes (Fig. 1C). Unsupervised hierarchical clustering of VILI and AIH samples based on the differentially expressed genes further showed that samples

belonging to the same cohort clustered together (Fig. 1D). Finally, we performed gene set enrichment analysis (GSEA) to identify biological processes characteristic of the VILI and AIH cohort (Fig. 1E and Table S6). We found that pathways related to immune response were overrepresented in the AIH cohort, in particular gene sets associated with interferon response (e.g. Hallmark Interferon-Gamma Response, Reactome Interferon Gamma Signalling, and Hallmark Interferon Alpha Response). In contrast, mitochondrial metabolism and oxidative stress-related pathways were overrepresented in the VILI cohort. Because we performed transcriptome analysis from bulk RNA, we could not determine the cell type responsible for the observed differences. However, it is known that drug-induced liver injury (DILI) results from mitochondrial toxicity and impairment of the oxidation-phosphorylation machinery in hepatocytes.<sup>27,28</sup> Therefore, we carried out spatial whole transcriptome analysis with the GeoMx platform (Nanostring, Seattle, USA) selecting arginase positive hepatocytes from periportal and centrilobular regions of VILI and AIH (Fig. S2A and B). We found 53 genes (38 upregulated and 15 downregulated) demonstrating a significant differential expression between the two cohorts (lfc  $>0.58$ ,  $p_{\text{adj}} < 0.05$ ) (Fig. S2C and Table S7). GSEA revealed that the same four oxidative phosphorylation or liver metabolism related gene sets, which were enriched in bulk-RNA sequencing, were also significantly enriched with the spatial transcriptomic analysis of hepatocytes (Fig. S2D and Table S8). Therefore, hepatocytes are the main cells responsible for the differences between both cohorts in mitochondrial toxicity and impairment of the oxidation-phosphorylation machinery.

In summary, our data suggest that although VILI and AIH are related based on their expression profiles, they have distinct differences in biological processes.

#### Immunoprofiling shows higher portal/periportal CD8<sup>+</sup> T cell infiltration but lower B cell infiltration in VILI

Next, we characterised the immune infiltrates in the biopsy tissue. First, we performed a cell type enrichment analysis with our RNA gene expression data by using the xCell web tool.<sup>29</sup> Interestingly, we observed a more enriched 'B cells' signature in patients with AIH in comparison with patients with VILI ( $p = 0.0048$ ); however, it did not reach significance after adjustment to multiple testing ( $p_{\text{adj}} = 0.1150$ ) (Fig. 2A). In contrast to B cells, no enrichment difference was observed between the two cohorts for the other immune cell signatures.

Thereafter, we carried out multiplex immunofluorescence with co-detection by indEXing (CODEX; Akoya Biosciences, Marlborough, USA)<sup>30</sup> on FFPE liver biopsies of our cohorts with sufficient remaining tissue, resulting in the analysis of five patients with VILI and seven patients with AIH. By using different immune markers simultaneously (Fig. S3A), we assessed the density and differential localisation of B and T cells within the portal and centrilobular region of the liver parenchyma (Fig. 2B and Fig. S3B). CD79a was used as a marker for B cells including plasma cells, CD20 for B cells, CD3, CD8, CD4, and FoxP3 for respective T effector and regulatory T cells. CD3-positive T cells showed overall the highest cell density and were slightly more prominent in the portal region than in the centrilobular region in both cohorts (Fig. 2C and Fig. S3C). CD3<sup>+</sup> CD8<sup>+</sup> T effector cells showed a trend for a higher density

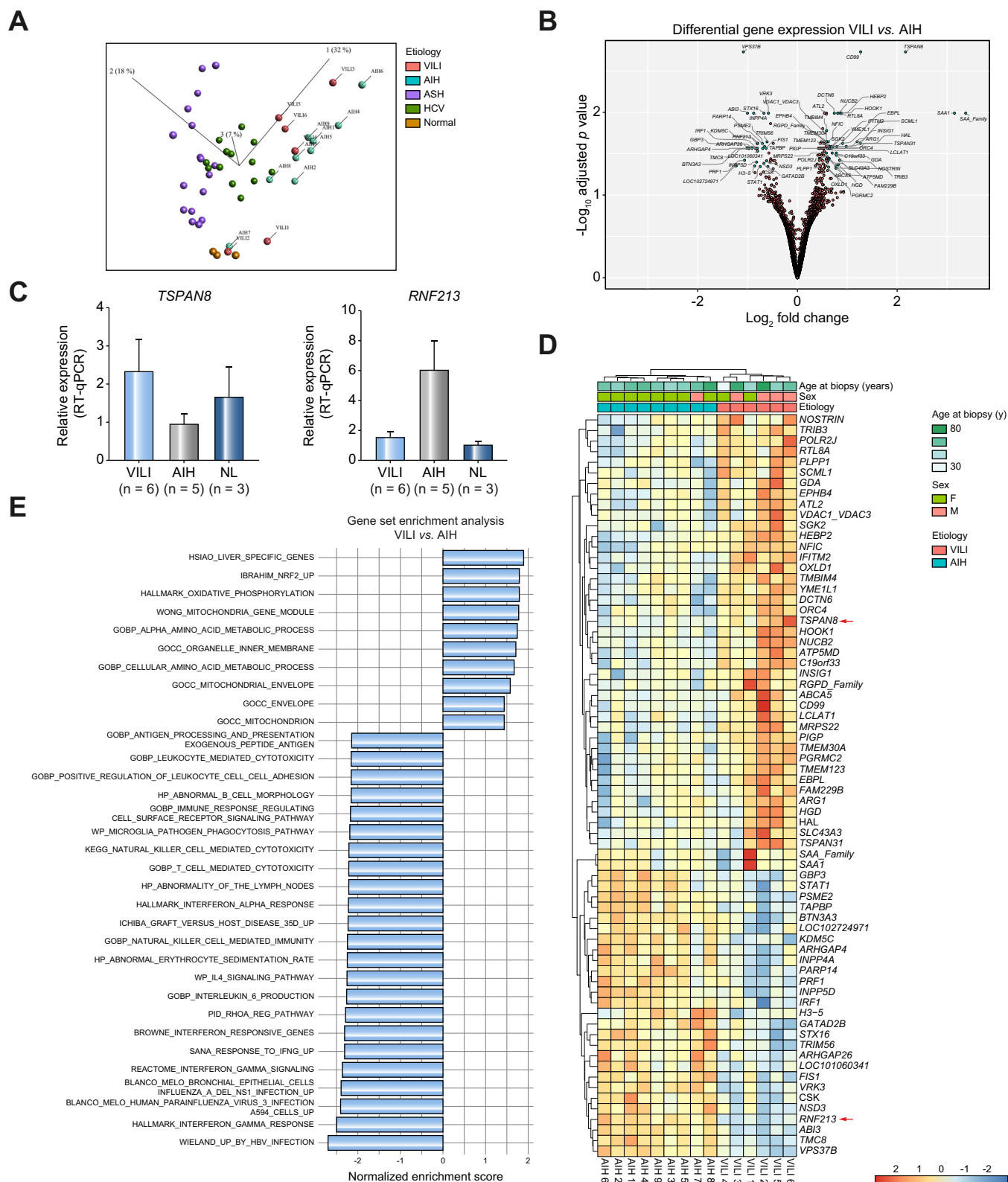


**Fig. 1. Whole transcriptome analysis reveals distinct differences between VILI and AIH.** (A) Principal component analysis of VILI (n = 6), AIH (n = 9), ASH (n = 17), HCV hepatitis (n = 13) and normal liver (n = 3). (B) Volcano plot for differentially expressed genes between VILI and AIH cohort. Genes with a  $\log_2$  fold change  $> 0.58$  and  $p_{\text{adj}} < 0.05$  were accepted as differentially expressed between cohorts. (C) qPCR result of *TSPAN8* and *RNF213* expression. VILI cohort, n = 6; AIH cohort, n = 5; normal liver, n = 3. (D) Unsupervised hierarchical clustering with differentially expressed genes between VILI and AIH samples. Arrows show the two genes which underwent validation of gene expression by qPCR. (E) Gene set enrichment analysis of VILI and AIH cohorts. Only pathways with  $p_{\text{adj}} < 0.05$  are shown. AIH, autoimmune hepatitis; ASH, alcoholic steatohepatitis; VILI, vaccine-induced liver injury.

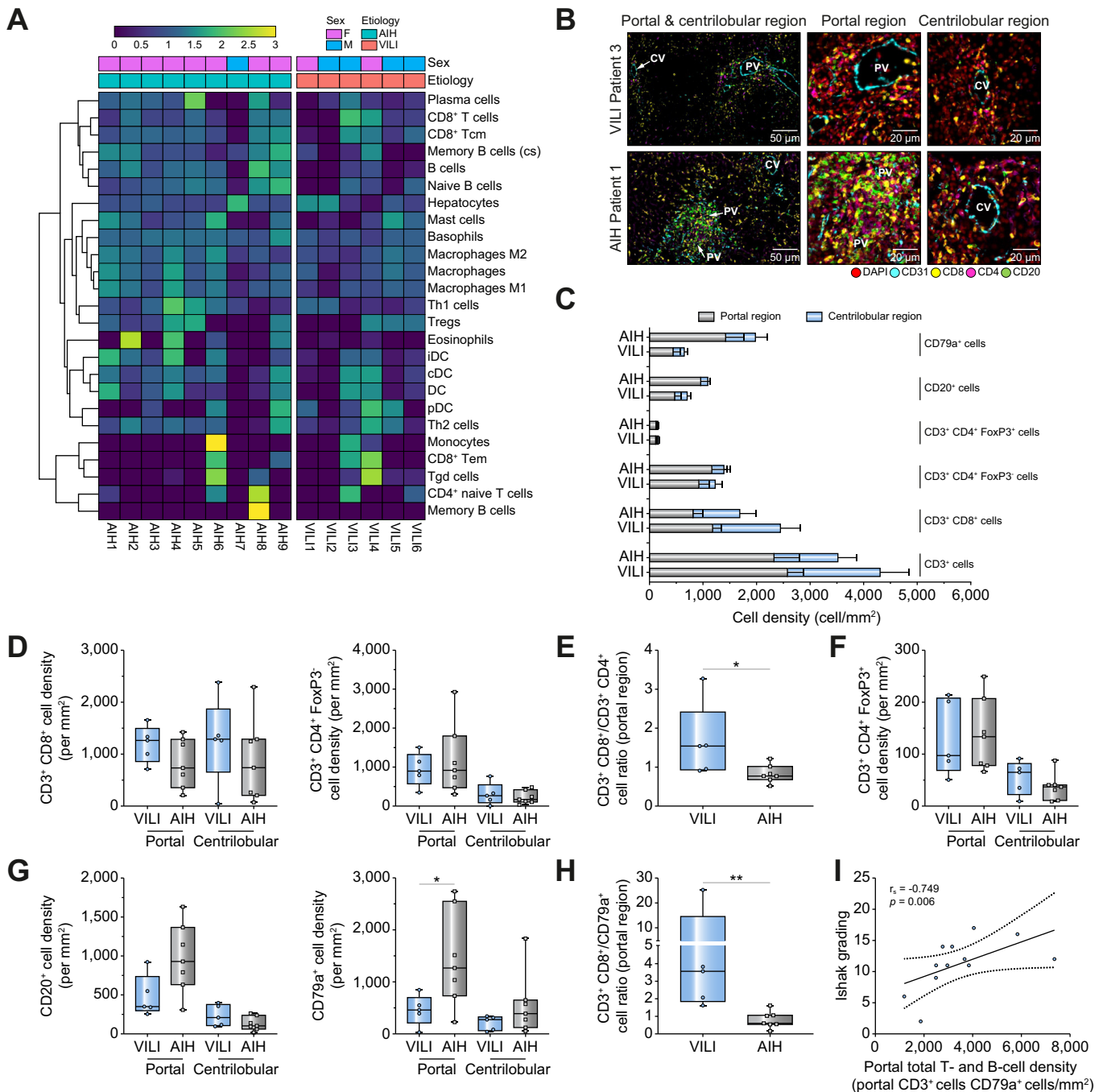


**Fig. 2. Immunophenotyping of VILI and AIH with xCell method and multiplex immunofluorescence.** (A) *In silico* immunophenotyping of VILI and AIH cases with xCell method. (B) Portal and centrilobular immune cell densities were quantified with CODEX multiplex immunofluorescence. (C) Immune cell distribution in the portal and centrilobular region of VILI and AIH samples. Bar graphs indicate mean and SEM of immune cell densities (cells/mm<sup>2</sup>). (D) CD3<sup>+</sup> CD8<sup>+</sup> and CD3<sup>+</sup> CD4<sup>+</sup> FoxP3<sup>+</sup> cell density in the portal and centrilobular region of VILI and AIH samples. (E) Ratio of CD3<sup>+</sup> CD8<sup>+</sup>/CD3<sup>+</sup> CD4<sup>+</sup> T cells in the portal region of VILI and AIH cohorts. (F) CD3<sup>+</sup> CD4<sup>+</sup> FoxP3<sup>+</sup> cell density in the portal and centrilobular region of VILI and AIH samples. (G) CD20<sup>+</sup> and CD79a<sup>+</sup> cell density in the portal and centrilobular region of VILI and AIH samples. (H) Ratio of CD3<sup>+</sup> CD8<sup>+</sup>/CD79a<sup>+</sup> T cells in the portal region of VILI and AIH cohorts. (I) Correlation analysis between Ishak grading and portal total T cell (CD3<sup>+</sup>) and B cell (CD79a<sup>+</sup>) density. The black line shows the linear regression line and dotted lines represent the 95% CI upper and lower limits. Each dot represents a patient. \* $p < 0.05$ , \*\* $p < 0.01$  (two-group comparison: Wilcoxon rank-sum test, correlation analysis: Spearman rank correlation test). AIH, autoimmune hepatitis; CV, central vein; PV, portal vein; VILI, vaccine-induced liver injury.

in VILI than in AIH in the portal (1264 vs. 734 cells/mm<sup>2</sup>) and centrilobular region (1288 vs. 739 cells/mm<sup>2</sup>), which did not reach significance (Fig. 2D). CD3<sup>+</sup> CD4<sup>+</sup> FoxP3<sup>+</sup> T effector cell density was similar between VILI and AIH in the portal (897 vs. 917 cells/mm<sup>2</sup>) and centrilobular region (265 vs. 170 cells/mm<sup>2</sup>,

Fig. 2D). Variability in immune cell density between patients within each cohort was high (Figs. S3C and S3D), which was already appreciated from the Ishak grading and whole transcriptome analysis described above. Therefore, we calculated the ratio between CD3<sup>+</sup> CD8<sup>+</sup> and CD3<sup>+</sup> CD4<sup>+</sup> effector T cells.

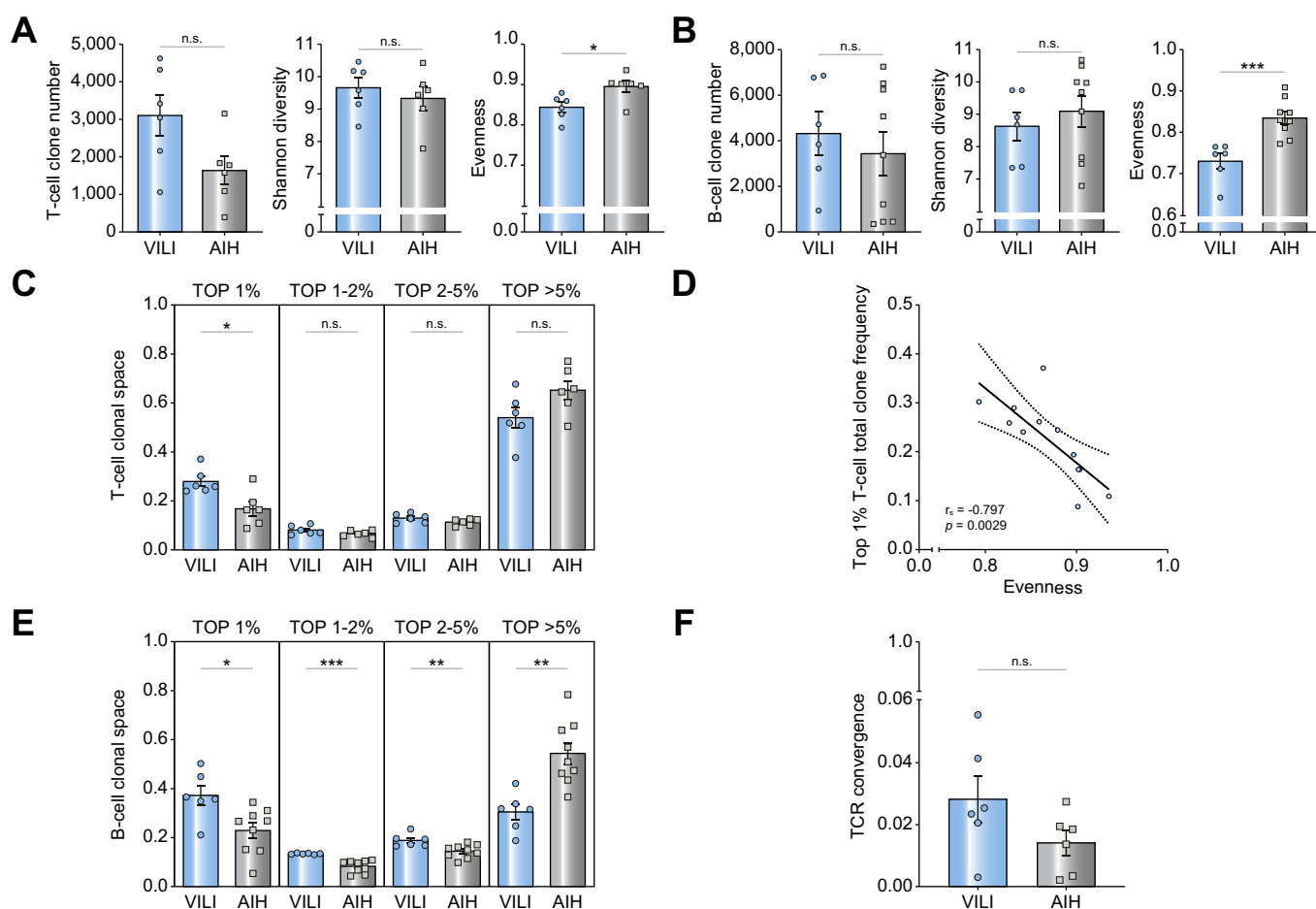


**Fig. 3. Global immune metrics and clonal space analysis of TCR and BCR repertoires of VILI and AIH.** (A) Global TCR repertoire metrics (clone number, Shannon diversity, evenness) of VILI ( $n = 6$ ) and AIH ( $n = 6$ ) patients. (B) Global BCR repertoire metrics (clone number, Shannon diversity, evenness) of VILI ( $n = 6$ ) and AIH ( $n = 9$ ) cohorts. (C) Clonal space occupied by T cell clones according to their frequency ranking. (D) Correlation of top 1% ranked total TCR frequency and evenness of VILI and AIH TCR repertoires. The black line shows the linear regression line and dotted lines represent the 95% CI upper and lower limits. (E) Clonal space occupied by B cell clones according to their frequency ranking. (F) TCR convergence of VILI and AIH cohorts. Each dot represents a patient. \* $p < 0.05$ , \*\* $p < 0.01$ , \*\*\* $p < 0.001$  (two-group comparison: unpaired Student  $t$  test, correlation analysis: Spearman rank correlation test). AIH, autoimmune hepatitis; BCR, B-cell receptor; ns, not significant; TCR, T-cell receptor; VILI, vaccine-induced liver injury.

Interestingly, the proportion of CD3<sup>+</sup> CD8<sup>+</sup> effector T cells in patients with VILI was significantly higher than in patients with AIH (1.541 vs. 0.7706;  $p = 0.0303$ ; Fig. 2E), indicating that the immune infiltrate in VILI was dominated by CD3<sup>+</sup> CD8<sup>+</sup> T cells.

Next, we analysed CD3<sup>+</sup> CD4<sup>+</sup> FoxP3<sup>+</sup> Treg cell distribution, which was similar in both cohorts (Fig. 2F). Finally, CD20<sup>+</sup> and CD79a<sup>+</sup> B cells both showed a lower density in VILI than in AIH in the portal region (CD20: 350.7 vs. 929.3 cells/mm<sup>2</sup>; CD79a<sup>+</sup>: 459.5 vs. 1267 cells/mm<sup>2</sup>), which reached significance for CD79a<sup>+</sup> B cells ( $p = 0.0480$ ) (Fig. 2G). In the centrilobular region, CD20<sup>+</sup> B cells were similar between both cohorts, but CD79a<sup>+</sup> B cells also showed a lower density in VILI than in AIH. Interestingly, we also observed a trend towards a positive correlation between portal CD79a<sup>+</sup> B cell density and serum IgG levels in VILI and AIH cases; however, it did not reach statistical significance ( $r_s = 0.639$ ,  $p = 0.052$ ) (Fig. S3E).

In conclusion, inflammation in VILI was dominated by CD8<sup>+</sup> effector T cells, whereas AIH showed a significantly higher portal infiltrate of CD79a<sup>+</sup> B cells and plasma cells. Indeed, the ratio of CD3<sup>+</sup> CD8<sup>+</sup> T effector cells to CD79a<sup>+</sup> B cells was significantly higher in VILI than in AIH (Fig. 2H). The total density of T and B

cells also correlated with Ishak grading ( $r_s = 0.749$ ,  $p = 0.006$ ) which indicated that our histopathological observations are in line with multiplex immunofluorescence analysis (Fig. 2I). In addition, we compared a small cohort ( $n = 4$ ) of DI-AILH with VILI and AIH. Liver histology, serology, and clinical characteristics of DI-AILH patients showed similarities with AIH (Tables S9 and S10). Two patients had a definite and two a probable AIH score according to the simplified AIH criteria.<sup>17</sup> Interestingly, the proportion of CD3<sup>+</sup> CD8<sup>+</sup> to CD3<sup>+</sup> CD4<sup>+</sup> effector T cells and CD3<sup>+</sup> CD8<sup>+</sup> to CD79a<sup>+</sup> B cells was higher in patients with DI-AILH than in patients with AIH (1.255 vs. 0.7706 and 6.316 vs. 0.6023) (Fig. S4), indicating that the composition of the immune infiltrate in DI-AILH is similar to VILI but different from AIH.

#### VILI cohort shows less evenness in TCR and BCR repertoire and larger clonal space of top 1% T cell clones

As a next step, we characterised the clonal distribution of the adaptive immune infiltrate in patients with VILI and AIH. We performed NGS-based immunoprofiling by sequencing the CDR3 region of the T-cell receptor (TCR) and B-cell receptor

(BCR) from bulk RNA isolated from liver biopsies. After applying stringent quality criteria, we obtained valid NGS data from all samples for BCR analysis ( $n = 15$ ), whereas TCR analysis was carried out with six samples from each cohort ( $n = 12$ ).

First, we started with the analysis of global immune repertoire metrics to assess clone number, diversity, and clonality as parameters for immunological complexity and for ongoing, successful, or deregulated immune response. Although VILI had increased T and B cell clone numbers, we did not find a significant difference between both cohorts (Fig. 3A and B). Moreover, the Shannon Diversity Index of both cohorts was similar in TCR and BCR repertoires. However, we found that VILI had significantly lower evenness in the TCR ( $p = 0.0212$ ) and BCR repertoire ( $p = 0.0008$ ), which indicated that VILI had more expanded clones in T and B cell architecture in comparison with AIH (Fig. 3A and B). Indeed, the spectratyping plots of T and B cell clone distribution in VILI samples showed few expanded T and B cell clones, suggesting a clonal expansion against specific antigens (Fig. S5A and B). In contrast, the clonal distribution of T and B cells was mainly composed of unexpanded clones in AIH samples, which suggested a more polyclonal reaction against antigenic stimulations (Fig. S5A and B). Next, we tested whether the evenness difference between the two cohorts arises specifically from the most abundant T and B cell clones in the liver tissues. For this purpose, we performed clonal space analysis that was previously used to determine which ranges of clones are associated with the TCR repertoire difference.<sup>32,33</sup> First, T and B cell clones were divided into four groups according to their ranked frequencies (top 1%, top 1–2%, top 2–5%, and >5%). Thereafter, the clone frequency in each group in relation to the total immune repertoire was calculated. As expected from the difference in evenness, we found that the T cell clones in the top 1% group of the VILI cohort had a significantly larger clonal space compared to the AIH cohort (27.9% vs. 16.8%;  $p = 0.0104$ ; Fig. 3C). This suggests that this group of T cells is the main responder against vaccination-related antigenic stimulation. In contrast, there was no difference in the top 1–2% and top 2–5%. Since the T cell architecture was dominated by the top 1% in VILI samples, the >5% group occupied a larger space in AIH compared with the VILI cohort, however, it did not reach significance (mean VILI vs. AIH: 54.0% vs. 65.1%,  $p = 0.0754$ ). We also tested whether the total frequency of top 1% T cell clones correlated with the evenness in each patient and found that these two parameters showed a significant inverse correlation with each other ( $r_s = -0.797$ ,  $p = 0.0029$ ; Fig. 3D). In the B cell compartment, the top 1%, top 1–2%, and top 2–5% had a significantly larger clonal space in the VILI cohort, whereas the >5% group occupied a larger space in AIH than in VILI (Fig. 3E). This highlights the more pronounced presence of a general B cell clone expansion in VILI samples and is consistent with the difference in evenness between VILI and AIH samples (Fig. 3E).

Next, we analysed in more detail the sharing of T cell clone sequences and their specificity. Of the 184 top 1% T cell clones from all six VILI liver samples, no shared clones were detected among them. Yet, when we uploaded the beta chain CDR3 sequences of the 184 top 1% liver T cell clones to a publicly available TCR database (<http://tools.iedb.org/tcrmatch/>), we found seven spike SARS-CoV-2 glycoprotein epitopes that matched with CDR3 sequences (Table S11), indicating that some high-frequency T cell clones may possibly recognise the

spike glycoprotein. For one patient (VILI #5), a blood sample was available from the time of liver biopsy. Therefore, we searched for shared T cell clones between the blood sample and the liver biopsy. Interestingly, of the 47 top 1% T cell clones of the liver, we found 13 shared T cell clones within the blood sample (Table S12). To further determine whether shared clones could represent SARS-CoV-2 spike-protein specific T cells, we analysed an additional patient (VILI\_F) recently published in a case report, who was found to have a CD8<sup>+</sup> T cell response against a pre-described Spike-protein epitope (S<sub>378-386</sub>) of SARS-CoV-2.<sup>9</sup> However, the number of sorted S<sub>378-386</sub> tetramer-positive cells from PBMCs, which represent only a fraction of the whole anti-Spike T cell response, was insufficient for following TCR sequencing. However, we were able to perform TCR sequencing from the S<sub>378-386</sub>-depleted fraction. Interestingly, all of the top 1% T cell clones ( $n = 10$ ) and 96% ( $n = 47$ ) of the top 50 most frequent T cell clones in the liver could be detected in PBMC-sorted spike-protein negative T cell clones (Table S13). Yet, none of the shared T cell clones between liver and blood of these two patients matched to the TCR database described above. Finally, we looked at TCR convergence which was suggested as an indicator of antigen-specific T cell response.<sup>31</sup> Although we observed a higher convergence in VILI samples, it did not reach significance (mean VILI vs. AIH: 2.8% vs. 1.4%;  $p = 0.1248$ ; Fig. 3F).

In conclusion, our data indicate that COVID-19 vaccination leads to the expansion of a unique set of T cells in the liver, many of which can also be detected in the blood.

#### Immune repertoires of VILI and AIH samples have an identical CDR3 length distribution but show variations in TCR beta variable-joining and immunoglobulin heavy chain variable-joining gene usage

The diversity of CDR3 length is one of the critical determinants of the antigen recognition process by T and B cells. Therefore, we compared CDR3 length distribution in both cohorts. VILI and AIH showed a similar CDR3 length distribution pattern with comparable mean CDR3 nucleotide length in both TCR (36.72 vs. 36.42; Fig. 4A) and BCR (45.78 vs. 46.76; Fig. 4B) repertoires. We next evaluated the variable and joining (V-J) region usage in TCR and BCR repertoires of VILI and AIH samples. As shown in Fig. 4C, T and B cell clones from different patients of the same cohort had a distinct pattern of TCR beta variable-joining (TRBV-J) and immunoglobulin heavy chain variable-joining (IGHV-J) usage and each sample had a different set of V-J genes, which was overrepresented or underrepresented. Previously, it was reported that TRBV6-1 and TRBV6-4 were used less frequently in patients with AIH compared with normal controls.<sup>32</sup> Accordingly, we observed that TRBV6-1 and TRBV6-4 genes were used less frequently in the AIH cohort compared with the VILI cohort; however, only TRBV6-1 was statistically significant (Fig. 4D). Besides, TRBV5-1 was significantly less and TRBV7-6 was significantly more frequently used in VILI in comparison with the AIH cohort (Fig. 4D). Only one gene from the IGH repertoire, IGHV1-24, displayed a significant usage difference and was found less frequently in the VILI cohort (Fig. 4E).

## Discussion

A growing body of evidence indicates a direct causality between COVID-19 vaccination and hepatitis in very rare cases

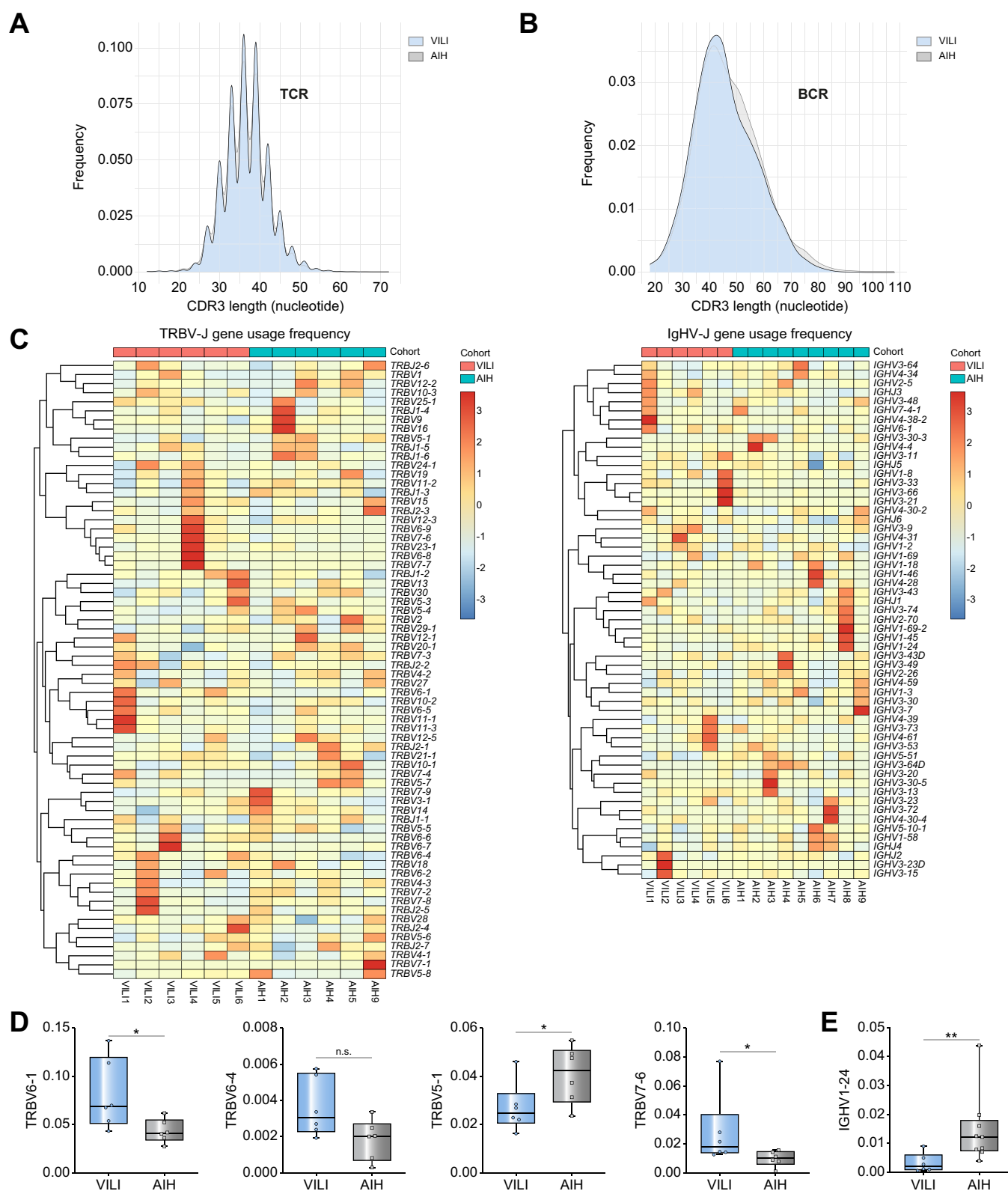


**Fig. 4. Identical CDR3 length distribution but variations in TRBV-J and IgHV-J gene usage between patients with VILI and AIH.** (A) CDR3 nucleotide length distribution of TCR repertoires of patients with VILI and AIH. (B) CDR3 nucleotide length distribution of BCR repertoires of VILI and AIH samples. (C) Heatmap of TCR- $\beta$  chain and BCR CDR3 region variable and joining gene usage proportion in each sample. (D) Preferential usage of TRBV6-1, TRBV6-4, TRBV5-1, and TRBV7-6. (E) Preferential usage of IGHV1-24 in patients with AIH. For TCR analysis six patients with VILI and six patients with AIH, for BCR analysis six patients with VILI and nine patients with AIH were included. Each dot represents a patient. \* $p < 0.05$ , \*\* $p < 0.01$ , \*\*\* $p < 0.001$  (two-group comparison: Wilcoxon rank-sum test). AIH, autoimmune hepatitis; BCR, B-cell receptor; CDR3, complementarity-determining region 3; IgHV-J, immunoglobulin heavy chain variable-jointing; ns, not significant; TCR, T-cell receptor; TRBV-J, T-cell receptor beta variable-jointing; VILI, vaccine-induced liver injury.

(summarised in Table S14).<sup>7–9</sup> The clinical, biochemical, histologic and partially serologic appearance of COVID-19 vaccine-induced hepatitis is similar to AIH.<sup>10,11</sup> However, it is unclear how these two diseases are related to each other. In addition, the pathophysiological mechanisms of COVID-19 vaccine-induced hepatitis are poorly understood, which prompted us to conduct this comparative study between VILI and AIH. All patients with VILI in our study showed a close temporal correlation between COVID-19 vaccination and hepatitis in the absence of other causes of acute liver injury. Although two patients were taking drugs potentially associated with liver injury (statin and lercanidipine/telmisartan), a causal relationship is unlikely, because these drugs usually cause liver toxicity within the first few weeks of use and our patients have been taking them for many years without previous adverse effects. Four of the six patients with VILI were ANA- or AAA-positive, including one with atypical AMA.<sup>6</sup> In addition, serum IgG levels were elevated in two patients. A total of 60% of our patients were classified as probable/definite AIH, according to the simplified criteria, which is only slightly lower than in previously published cohorts of VILI.<sup>15</sup> In contrast, all patients with AIH in our cohort had either ANA and/or ASMA/AAA and were all classified as probable/definite AIH according to the simplified criteria. Importantly, all patients with VILI responded well to steroid therapy or improved without therapy and remained in remission to date.

H&E morphology was very similar between VILI and AIH. A significant difference was found only in confluent necrosis, which was more extensive in VILI. Similarly, a previous report revealed a higher zone 3 necrosis in DI-AILH compared with AIH.<sup>33</sup> Interestingly, we found no difference between the two groups for eosinophilic infiltrates, a finding often associated with DILI.<sup>33,34</sup> Whole transcriptome analysis confirmed the close relationship between VILI and AIH. However, GSEA also revealed an overrepresentation of mitochondrial metabolism and oxidative stress-related pathways in VILI compared with AIH. These pathways have been mapped to hepatocytes and are important in DILI<sup>27,28</sup> and may indicate immunopathological similarities between VILI and DI-AILH. In contrast, we found an increase in pathways related to interferon-gamma signalling in AIH compared with VILI. Indeed, it is well known that interferon pathways are activated in AIH.<sup>35,36</sup> Interestingly, this interferon response still appears to be significantly higher in AIH than in VILI, although mRNA-based vaccination can also elicit interferon signalling.<sup>37</sup> Furthermore, VILI and AIH were clearly separated from patients with chronic HCV infection or ASH. However, this may be partly explained by the fact that patients with chronic HCV and ASH in our cohort had cirrhosis, which was not present in VILI and AIH.

Cellular analysis of liver inflammation by transcriptome analysis and multiplex immunofluorescence further showed that VILI was dominated by CD8<sup>+</sup> effector T cells, whereas CD4<sup>+</sup> effector T cells and B/plasma cells were more prominent in AIH. This is in line with earlier reports showing that activated cytotoxic CD8<sup>+</sup> T cells were highly enriched in the liver of patients with VILI.<sup>9</sup> Interestingly, we observed a similar dominance of CD8<sup>+</sup> effector T cells in DI-AILH, suggesting that VILI and DI-AILH are closely related and distinct from AIH.

TCR and BCR analysis revealed similar clone numbers and Shannon Diversity Index between VILI and AIH. Yet, we found that VILI had lower evenness in the TCR and BCR repertoires, indicating that VILI has expanded clones in T and B cell architecture compared with AIH. Therefore, vaccination induces a more restricted repertoire, as indicated by the increase of T cell clones in the top 1% of VILI. Additionally, we compared T cell clones from the liver biopsy of two patients with VILI with matched blood samples. Interestingly, many of the high frequency T cell clones in the liver were also found in the blood of the same patient. However, none of these shared clones matched to spike SARS-CoV-2 in a TCR database. Moreover, we observed a clonal overlap in the patient in whom CD8<sup>+</sup> T cells specific for a spike protein epitope (S<sub>378–386</sub>) were depleted from PBMC.<sup>9</sup> Therefore, our data suggest that T cell clones that do not target a vaccine antigen may be involved in the pathogenesis of VILI. However, we cannot determine whether these high frequency T cells are activated in the liver and then spill over into the periphery or whether T cells from the periphery home to the liver to cause hepatitis.

Interestingly, in our gene usage analysis, we found a decrease in the rearranged TRBV6-1 and TRBV6-4 genes in AIH, in contrast to VILI. This is in line with earlier analysis of AIH, where also a decrease of TRBV6-1 and TRBV6-4 genes has been described.<sup>32</sup> The preferential usage of TRBV6 and TRBV20 family gene variants is a key feature of different subsets of mucosal associated invariant T (MAIT) cells.<sup>38,39</sup> Loss of MAIT cell subsets in the peripheral blood has been reported in a variety of autoimmune diseases and may be a characteristic for AIH. Furthermore, we observed a decrease in IGHV1-24 in VILI compared with AIH. In contrast, previous studies observed an enrichment of IGHV1-24 in B cell repertoires<sup>40,41</sup> after SARS-CoV-2 infection. However, no enrichment in IGHV1-24 was observed in IgH repertoires of healthy individuals after SARS-CoV-2 vaccination.<sup>42</sup>

COVID-19 vaccination is the most effective measure to prevent spreading and reduce mortality after SARS-CoV-2 infection. Moreover, the risk of liver injury during COVID-19 disease by far outweighs the risk of liver injury after vaccination.<sup>43</sup> Therefore, we strongly advocate vaccination during the pandemic. However, we need to be cautious of hepatitis as a rare side effect of vaccination and understand VILI better. We are aware of the rather small sample size of our study. However, besides some similarities between VILI and AIH, we found distinct differences between the two entities. TRBV-J gene usage showed that TRBV6-1 and TRBV6-4 were reduced only in the cohort with AIH, which has been described as typical for AIH.<sup>32</sup> Immune infiltration in VILI was also dominated by CD8<sup>+</sup> effector T cells, whereas CD4<sup>+</sup> effector T cells and CD79a<sup>+</sup> B and plasma cells were prominent in AIH. Mitochondrial metabolism and oxidative stress-related pathways were further upregulated in the cohort with VILI, in parallel with a more pronounced centrilobular necrosis. Although we cannot exclude that some VILI represent activation of latent AIH, our results suggest that in many individuals, VILI represents a separate disease entity, which is distinct from AIH, but more closely related to DI-AILH. Therefore, there is a good chance that many patients with VILI will recover completely and not develop long-term AIH.

## Affiliations

<sup>1</sup>Institute of Pathology, University Hospital Basel, Basel, Switzerland; <sup>2</sup>Microscopy Core Facility, Department of Biomedicine, University of Basel, Basel, Switzerland; <sup>3</sup>Center for Virology and Vaccine Research, Beth Israel Deaconess Medical Center, Boston, MA, USA; <sup>4</sup>Department of Medicine II (Gastroenterology, Hepatology, Endocrinology and Infectious Diseases), Freiburg University Medical Center, Faculty of Medicine, University of Freiburg, Freiburg, Germany; <sup>5</sup>Faculty of Biology, University of Freiburg, Freiburg, Germany; <sup>6</sup>Institute for Surgical Pathology, Freiburg University Medical Center, University of Freiburg, Freiburg, Germany; <sup>7</sup>Core Facility for Histopathology and Digital Pathology, Medical Center, Faculty of Medicine, University of Freiburg, Freiburg, Germany; <sup>8</sup>Istituto Cantonale di Patologia, Locarno, Switzerland; <sup>9</sup>Innere Medizin, Spital Dornach, Dornach, Switzerland; <sup>10</sup>Department of Biomedical Sciences, Humanitas University, Pieve Emanuele, Milan, Italy; <sup>11</sup>IRCCS Humanitas Research Hospital, Rozzano, Milan, Italy; <sup>12</sup>Brain Tumor Immunotherapy Lab, Department of Biomedicine, University of Basel, Basel, Switzerland; <sup>13</sup>Department of Neurosurgery, University Hospital Basel, Basel, Switzerland; <sup>14</sup>Gastroenterology and Hepatology, University Centre for Gastrointestinal and Liver Diseases Basel, Switzerland; <sup>15</sup>Signalling Research Centres BIOS and CIBSS, University of Freiburg, Freiburg, Germany; <sup>16</sup>Partner Site Freiburg, German Cancer Consortium (DKTK), Heidelberg, Germany; <sup>17</sup>Department of Biomedicine, University of Basel, Switzerland; <sup>18</sup>Department of Pathology, Dana Farber Cancer Institute, Boston, MA, USA; <sup>19</sup>Broad Institute of Harvard and MIT, Cambridge, MA, USA; <sup>20</sup>Faculty of Biomedical Sciences, Università Della Svizzera Italiana, Lugano, Switzerland; <sup>21</sup>Epatocentro Ticino, Lugano, Switzerland; <sup>22</sup>MowatLabs, Faculty of Life Sciences and Medicine, King's College London, King's College Hospital, London, UK

## Abbreviations

AAAs, anti-actin antibodies; AIH, autoimmune hepatitis; ALP, alkaline phosphatase; ALT, alanine aminotransferase; AMAs, anti-mitochondrial antibody; ANAs, anti-nuclear antibody; ANCAs, anti-neutrophil cytoplasm antibodies; Anti-LC1, anti-liver cytosol type 1; Anti-LKM1, anti-liver-kidney microsome 1; Anti-SLA, anti-soluble liver antigen; ASMAs, anti-smooth muscle antibodies; ASH, alcoholic steatohepatitis; AST, aspartate aminotransferase; BCR, B-cell receptor; CDR3, complementarity-determining region 3; CODEX, CO-Detection by IndEXing; COVID-19, coronavirus disease 2019; DI-AIH, drug-induced autoimmune-like hepatitis; DILI, drug-induced liver injury; FFPE, formalin-fixed and paraffin-embedded; GGT, gamma-glutamyltransferase; GSEA, gene set enrichment analysis; IgH, immunoglobulin heavy chain; IgHV-J, immunoglobulin heavy chain variable-joining; lfc, log fold change; MAIT, mucosal associated invariant T; SARS-CoV-2, severe acute respiratory syndrome coronavirus 2; TCR, T-cell receptor; TRBV-J, T-cell receptor beta variable-joining; ULN, upper limit of normal; VILI, vaccine induced liver injury.

## Financial support

This study was funded by the Botnar Research Centre for Child Health (FTC-2020-10) to AT, MSM, and GH and the Swiss National Science Foundation (SNSF; Grant No. 320030\_189275) to MSM. SJ is supported by NIH DP2AI171139, and the Bill & Melinda Gates Foundation INV-002704. The sponsor of the study did not have any role in the study design, or collection, analysis, and interpretation of data.

## Conflicts of interest

MSM has served as a consultant for ThermoFisher, Merck, GlaxoSmithKline, Janssen-Cilag, Roche, and Novartis and received speaker's honorarium from Incyte Biosciences. GH is cofounder of Incephalo, not related to this project. Otherwise, the authors have no conflicts of interest to declare.

Please refer to the accompanying ICMJE disclosure forms for further details.

## Authors' contributions

Conceptualisation: SU, MSM. Methodology: SU, MSM, ACB, EMB, SJ, CZ. Clinical data and patient integration: SU, MSM, JH, JV, LM, MM, IP, TH, LMT, AT, MH, CB, BTBP. Sample handling and processing: SU, ACB, CZ, IA, EMB, MM, IP, BC, MR, PB, AKS, JH, JV, LM, TH, LMT, AT, TB, MH, BB, MHH, CB, BTBP, MSM. Software: SU, ACB, CZ, IA, EMB. Formal analysis: SU, ACB, CZ, JY, IA, EMB, AKS, JH, JV, LM, TH, LMT, AT, MH, SJ, CB, BTBP, MSM. Investigation: SU, ACB, CZ, IA, EMB, JY, SJ, MSM. Resources: AT, MSM. Writing – original draft: SU, MSM. Writing – review and editing: all authors. Supervision: SU, MSM. Project administration: AKS, AT, MSM. Funding acquisition: AT, MSM, GH, SJ.

## Data availability statement

The data of this study are available in Gene Expression Omnibus (<https://www.ncbi.nlm.nih.gov/geo/>) under GEO accession number GSE229459.

## Acknowledgements

We would like to thank Jan Schneeberger for excellent technical assistance. We thank Dr Stéphanie Tissot and Dr Jonathan Thevenet from the Immune

Landscape Laboratory of University Hospital of Lausanne for their support in GeoMx experiment and spatial transcriptome sequencing.

## Supplementary data

Supplementary data to this article can be found online at <https://doi.org/10.1016/j.jhep.2023.05.020>.

## References

*Author names in bold designate shared co-first authorship.*

- [1] WHO Coronavirus (COVID-19) Dashboard, <https://covid19.who.int/>. Access Date 27 June 2023.
- [2] **Li M, Wang H, Tian L, Pang Z, Yang Q, Huang T, et al.** COVID-19 vaccine development: milestones, lessons and prospects. *Signal Transduct Target Ther* 2022;7:146.
- [3] **Bril F, Al Daffal S, Dean M, Fettig DM.** Autoimmune hepatitis developing after coronavirus disease 2019 (COVID-19) vaccine: causality or casualty? *J Hepatol* 2021;75:222–224.
- [4] **Rocco A, Sgamato C, Compare D, Nardone G.** Autoimmune hepatitis following SARS-CoV-2 vaccine: may not be a casualty. *J Hepatol* 2021;75:728–729.
- [5] **Londono MC, Gratacos-Gines J, Saez-Penataro J.** Another case of autoimmune hepatitis after SARS-CoV-2 vaccination – still casualty? *J Hepatol* 2021;75:1248–1249.
- [6] **Ghielmetti M, Schaufelberger HD, Mieli-Vergani G, Cerny A, Dayer E, Vergani D, et al.** Acute autoimmune-like hepatitis with atypical anti-mitochondrial antibody after mRNA COVID-19 vaccination: a novel clinical entity? *J Autoimmun* 2021;123:102706.
- [7] **Zin Tun GS, Gleeson D, Al-Joudeh A, Dube A.** Immune-mediated hepatitis with the Moderna vaccine, no longer a coincidence but confirmed. *J Hepatol* 2022;76:747–749.
- [8] **Garrido I, Lopes S, Simoes MS, Rodrigo L, Lopes J, Carneiro F, et al.** Autoimmune hepatitis after COVID-19 vaccine – more than a coincidence. *J Autoimmun* 2021;125:102741.
- [9] **Boettler T, Csernalabics B, Salie H, Luxenburger H, Wischer L, Alize ES, et al.** SARS-CoV-2 vaccination can elicit a CD8 T-cell dominant hepatitis. *J Hepatol* 2022;77:653–659.
- [10] **Codoni G, Kirchner T, Engel B, Villamil AM, Efe C, Stättermayer AF, et al.** Histological and serological features of acute liver injury after SARS-CoV-2 vaccination. *JHEP Rep* 2023;5:100605.
- [11] **Efe C, Kulkarni AV, Terziroli Beretta-Piccoli B, Magro B, Stättermayer A, Cengiz M, et al.** Liver injury after SARS-CoV-2 vaccination: features of immune-mediated hepatitis, role of corticosteroid therapy and outcome. *Hepatology* 2022;76:1576–1586.
- [12] **Kanduc D, Shoenfeld Y.** Molecular mimicry between SARS-CoV-2 spike glycoprotein and mammalian proteomes: implications for the vaccine. *Immunol Res* 2020;68:310–313.
- [13] **Vojdani A, Kharrazian D.** Potential antigenic cross-reactivity between SARS-CoV-2 and human tissue with a possible link to an increase in autoimmune diseases. *Clin Immunol* 2020;217:108480.
- [14] **Avci E, Abasiyanik F.** Autoimmune hepatitis after SARS-CoV-2 vaccine: new-onset or flare-up? *J Autoimmun* 2021;125:102745.

- [15] Roy A, Verma N, Singh S, Pradhan P, Taneja S, Singh M. Immune-mediated liver injury following COVID-19 vaccination: a systematic review. *Hepatol Commun* 2022;6:2513–2522.
- [16] Manns MP, Czaja AJ, Gorham JD, Krawitt EL, Mieli-Vergani G, Vergani D, et al. Diagnosis and management of autoimmune hepatitis. *Hepatology* 2010;51:2193–2213.
- [17] Hennes EM, Zeniya M, Czaja AJ, Dalekos GN, Krawitt EL, Bittencourt PL, et al. Simplified criteria for the diagnosis of autoimmune hepatitis. *Hepatology* 2008;48:169–176.
- [18] Björnsson ES, Medina-Caliz I, Andrade RJ, Lucerna MI. Setting up criteria for drug-induced autoimmune-like hepatitis through a systematic analysis of published reports. *Hepatol Commun* 2022;6:1895–1909.
- [19] Fimiano F, D'Amato D, Gambella A, Marzano A, Saracco GM, Morgando A. Autoimmune hepatitis or drug-induced autoimmune hepatitis following Covid-19 vaccination? *Liver Int* 2022;42:1204–1205.
- [20] Chen Y, Xu Z, Wang P, Li X, Shuai Z, Ye D, et al. New-onset autoimmune phenomena post-COVID-19 vaccination. *Immunology* 2022;165:386–401.
- [21] Fontana RJ, Seeff LB, Andrade RJ, Björnsson E, Day CP, Serrano J, et al. Standardization of nomenclature and causality assessment in drug-induced liver injury: summary of a clinical research workshop. *Hepatology* 2010;52:730–742.
- [22] Tiniakos DG, Brain JG, Bury YA. Role of histopathology in autoimmune hepatitis. *Dig Dis* 2015;33(Suppl. 2):53–64.
- [23] Lohse AW, Sebode M, Bhathal PS, Clouston AD, Dienes HP, Jain D, et al. Consensus recommendations for histological criteria of autoimmune hepatitis from the international AIH Pathology group: results of a workshop on AIH histology hosted by the European reference network on hepatological diseases and the European society of Pathology. *Liver Int* 2022;42:1058–1069.
- [24] Ishak K, Baptista A, Bianchi L, Callea F, Groote JD, Gudat F, et al. Histological grading and staging of chronic hepatitis. *J Hepatol* 1995;22:696–699.
- [25] Hysenaj L, Little S, Kulhanek K, Gbenedio OM, Rodriguez L, Shen A, et al. SARS-CoV-2 infection studies in lung organoids identify TSPAN8 as novel mediator. *bioRxiv* 2021. <https://doi.org/10.1101/2021.06.01.446640>.
- [26] Pollaci G, Gorla G, Potenza A, Carrozzini T, Canavero I, Bersano A, et al. Novel multifaceted roles for RNF213 protein. *Int J Mol Sci* 2022;23:4492.
- [27] Mihajlovic M, Vinken M. Mitochondria as the target of hepatotoxicity and drug-induced liver injury: molecular mechanisms and detection methods. *Int J Mol Sci* 2022;23:3315.
- [28] Yuan L, Kaplowitz N. Mechanisms of drug-induced liver injury. *Clin Liver Dis* 2013;17:507–518 vii.
- [29] Aran D, Hu Z, Butte AJ. xCell: digitally portraying the tissue cellular heterogeneity landscape. *Genome Biol* 2017;18:220.
- [30] Black S, Phillips D, Hickey JW, Kennedy-Darling J, Venkataaraman VG, Samusik N, et al. CODEX multiplexed tissue imaging with DNA-conjugated antibodies. *Nat Protoc* 2021;16:3802–3835.
- [31] Pan MY, Li B. T cell receptor convergence is an indicator of antigen-specific T cell response in cancer immunotherapies. *eLife* 2022;11:e81952.
- [32] Schultheiss C, Simnica D, Willscher E, Oberle A, Fanchi L, Bonzanni N, et al. Next-generation immunosequencing reveals pathological T-cell architecture in autoimmune hepatitis. *Hepatology* 2021;73:1436–1448.
- [33] Qu LM, Wang SH, Yang K, Brigstock DR, Sun L, Gao R, et al. CD4(+) Foxp3(+)CD25(+) Tregs characterize liver tissue specimens of patients suffering from drug-induced autoimmune hepatitis: a clinical-pathological study. *Hepatobiliary Pancreat Dis Int* 2018;17:133–139.
- [34] Suzuki A, Brunt EM, Kleiner DE, Miquel R, Smyrk TC, Andrade RJ, et al. The use of liver biopsy evaluation in discrimination of idiopathic autoimmune hepatitis versus drug-induced liver injury. *Hepatology* 2011;54:931–939.
- [35] Terziroli Beretta-Piccoli B, Mieli-Vergani G, Vergani D. Autoimmune hepatitis. *Cell Mol Immunol* 2022;19:158–176.
- [36] Liberal R, de Boer YS, Heneghan MA. Established and novel therapeutic options for autoimmune hepatitis. *Lancet Gastroenterol Hepatol* 2021;6:315–326.
- [37] Arunachalam PS, Scott MKD, Hagan T, Li C, Feng Y, Wimmers F, et al. Systems vaccinology of the BNT162b2 mRNA vaccine in humans. *Nature* 2021;596:410–416.
- [38] Reantragoon R, Corbett AJ, Sakala IG, Gherardin NA, Furness JB, Chen Z, et al. Antigen-loaded MR1 tetramers define T cell receptor heterogeneity in mucosal-associated invariant T cells. *J Exp Med* 2013;210:2305–2320.
- [39] Lepore M, Kalinichenko A, Colone A, Paleja B, Singhal A, Tschumi A, et al. Parallel T-cell cloning and deep sequencing of human MAIT cells reveal stable oligoclonal TCRbeta repertoire. *Nat Commun* 2014;5:3866.
- [40] Voss WN, Hou YJ, Johnson NV, Delidakis G, Kim JE, Javanmardi K, et al. Prevalent, protective, and convergent IgG recognition of SARS-CoV-2 non-RBD spike epitopes. *Science* 2021;372:1108–1112.
- [41] Nielsen SCA, Yang F, Jackson KJL, Ramona AH, Röltgen K, Jean GH, et al. Human B cell clonal expansion and convergent antibody responses to SARS-CoV-2. *Cell Host Microbe* 2020;28:516–525.e5.
- [42] Kotagiri P, Mescia F, Rae WM, Bergamaschi L, Tuong ZK, Turner L, et al. B cell receptor repertoire kinetics after SARS-CoV-2 infection and vaccination. *Cell Rep* 2022;38:110393.
- [43] Wong CKH, Mak LY, Au ICH, Lai FTT, Li X, Wan EYFW, et al. Risk of acute liver injury following the mRNA (BNT162b2) and inactivated (CoronaVac) COVID-19 vaccines. *J Hepatol* 2022;77:1339–1348.